Sensors & Actuators: B. Chemical 381 (2023) 133451

Contents lists available at ScienceDirect

Sensors and Actuators: B. Chemical

journal homepage: www.elsevier.com/locate/snb

Wearable molecularly imprinted electrochemical sensor with integrated nanofiber-based microfluidic chip for in situ monitoring of cortisol in sweat

Xuecui Mei [a,b,1], Jiao Yang [a,1], Xinge Yu [c], Zhengchun Peng [d], Guanghui Zhang [e,*], Yingchun Li [a,b,d,**]

[a] School of Science, Harbin Institute of Technology, Shenzhen 518055, China
[b] School of Chemistry and Chemical Engineering, Harbin Institute of Technology, Harbin 150001, China
[c] Department of Biomedical Engineering, City University of Hong Kong, 999077, Hong Kong, China
[d] College of Optoelectronic Engineering, Shenzhen University, Shenzhen 518060, China
[e] Department of Laboratory Medicine, Shenzhen Hengsheng Hospital, Shenzhen, Guangdong 518102, China

ARTICLE INFO

Keywords:
Wearable sensor
Molecularly imprinted polymer
Electrochemical sensing
Nanofiber-based microfluidic chip
Sweat cortisol

ABSTRACT

Wearable sweat sensors are highly desirable for noninvasive monitoring of personal health. Herein, we developed a flexible electrochemical sensor based on nanofiber-involved microfluidic technique and molecularly imprinted polymer (MIP) for in situ and real-time sweat analysis. The sensor with polyethylene terephthalate (PET) as the substrate consisted of two layers, a bottom MIP-modified electrode layer for sensing and an upper nanofiber-based microfluidic layer for spontaneous sweat pumping. To enhance stability and sensitivity of the sensor, porous and interconnected 3D carbon nanofiber membrane decorated with gold nanoparticles (GnPs@CnFM) served as a matrix for MIP deposition. Prussian blue nanoparticles (PBnPs) as a "built-in" redox probe were embedded into MIP skeleton, enabling in situ monitoring of sweat substance. On the microfluidic layer, the super-hydrophilic and porous nanofibers allowed sweat to be automatically and rapidly pumped to the bottom sensing chamber. On the basis of the above, the sensor demonstrated a wide detection range of 1 nM~1 μM as well as excellent selectivity and stability with cortisol as the model analyte. On-body applicability of the sensor was also validated by real-time monitoring of cortisol in healthy volunteers' sweat.

1. Introduction

People living in modern fast-paced lifestyles inevitably suffer from long-term psychological and physical stress. Exposure to stress can cause the dysregulation of hormones in the body, which is thought to negatively affect health [1]. Cortisol is a steroid hormone released by the adrenal cortex and recognized as a stress hormone playing a major role in physiological processes [2–4]. Cortisol can be found in a variety of body fluids, including sweat, saliva, blood, and so on [5,6]. Among these fluids, sweat can be non-invasively extracted and continuously collected from various body sites, and thus personal health status can be assessed by monitoring biomarkers in sweat [7,8]. The normal concentration of cortisol in sweat is in the range of 0.02 ~ 0.5 μM [9,10], and its peak level usually occurs in the morning while the lowest at night [11,12]. Elevated cortisol levels in the body are linked to anxiety, depression, hypertension, cardiovascular diseases, diabetes, weakened immune system, post-traumatic stress disorder (PTSD), *etc*. [11,13,14], while low levels can cause Addison's disease [15,16]. Thus, rapid, accurate and reliable measurement of cortisol is of great significance for personal stress management and clinical diagnosis [17,18].

Several techniques have been developed for sweat cortisol detection, such as high-performance liquid chromatography (HPLC), enzyme-linked immunosorbent assay (ELISA), lateral flow assay and electrochemical immunosensing [4,18–20]. Although these methods feature high accuracy and sensitivity, they are usually laborious, time-consuming and expensive [16,18]. Moreover, enzyme/antibody/aptamer-based detection devices tend to be environmentally unstable and thus have a short shelf-life [21]. Molecularly imprinted polymer (MIP) is a versatile biomimetic molecular receptor, which acts as an artificial antibody with the advantages of

* Corresponding author.
** Corresponding author at: School of Science, Harbin Institute of Technology, Shenzhen 518055, China.
E-mail addresses: zghui999@163.com (G. Zhang), liyingchun@hit.edu.cn (Y. Li).
[1] Xuecui Mei and Jiao Yang contributed equally to this work.

https://doi.org/10.1016/j.snb.2023.133451
Received 22 December 2022; Received in revised form 28 January 2023; Accepted 30 January 2023
Available online 1 February 2023

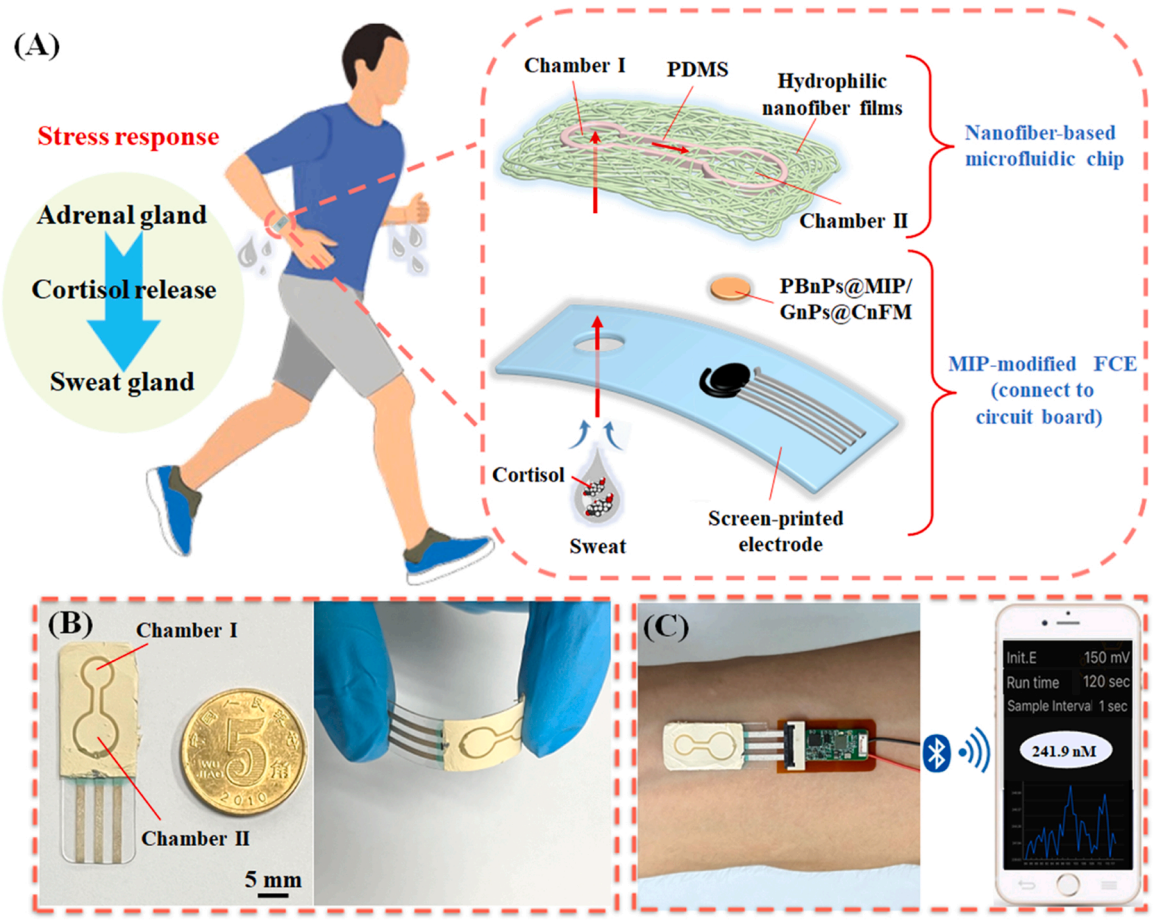

Fig. 1. Schematic illustration of the sensor for cortisol analysis. (A) Schematic representation of the layered sensor. (B) Photographs of the sensor in a flat and a bent state. (C) The sensor integrated with a flexible circuit board on a volunteer's wrist.

predetermined selectivity, excellent stability, cost-effectiveness and ease of preparation [10,22,23]. MIPs have been applied for the specific recognition of various biomarkers in biofluids, showing eximious performances [23–25]. Therefore, introduction of MIP to extract targets from sweat has become a promising alternative. On the other hand, in the fast-evolving world, modern self-health monitoring and management as well as personalized healthcare pay more attention to miniaturization, portability, comfort and intelligence of devices. Wearable microfluidic devices represent an emerging technique and have begun unlocking new insights for personalized physiological state monitoring [8,26]. Such devices that integrated with microfluidic chips, sensing units, signal processing and transmission electronics can be conformally worn on the surface of human skin, making them ideal for hassle-free, non-invasive and real-time analysis of markers in sweat [27,28]. Among them, microfluidic chips offer a promising pathway for sweat sampling, which can spontaneously collect sweat and transport it to sensing regions, playing a very important role in wearable devices [29, 30]. At present, most microfluidic chips involve expensive instruments and complex fabrication processes [31,32]. In comparison, electrospun nanofibers have the merits of simple preparation, excellent flexibility and tunable materials composition [33,34], which are very suitable for construction of flexible microfluidic chips. To the best of our knowledge, nanofiber-based microfluidic chips have not been reported.

In this paper, we demonstrate for the first time the amalgamation of molecularly imprinted electrochemical sensor and nanofiber-based microfluidic chips toward the realization of in situ and real-time monitoring of sweat cortisol. Prussian blue nanoparticles (PBnPs) embedded MIP (PBnPs@MIP) membrane prepared on screen-printed flexible carbon electrodes (FCE) by electro-polymerization provides the sensor with specific imprinted cavities, which can accurately capture cortisol molecules. Particularly, PBnPs, as "built-in" redox probes, were decorated in the MIP membrane during the electro-polymerization, realizing in situ detection of cortisol. Moreover, to improve sensitivity, carbon nanofiber membrane decorated with gold nanoparticles (GnPs@CnFM) were utilized to modify the FCE, endowing the sensor with high stability and sensitivity due to its large surface area, high porosity, interconnected three-dimensional (3D) construction and excellent electrical properties. What's more, the newly developed nanofiber-based microfluidic chip could automatically collect sweat from human skin and route it to the surface of the PBnPs@MIP-based electrode for sensing. The presented sensor determined cortisol with low detection limit and exhibited excellent performance in view of rapidity and reliability. This sensor was further connected to a wireless flexible circuit board for in situ signal processing, which allowed data to be passed directly to the user via Bluetooth. Besides, the device enabled real-time quantitative detection of sweat cortisol in on-body test, and the results were validated by commercial ELISA.

2. Experimental

2.1. Preparation of PBnPs@MIP/GnPs@CnFM/FCE

Fabrication procedures of the flexible sensor was illustrated in Fig. S1. Firstly, a flexible PET substrate was patterned by a laser cutting method. Then, a three-electrode system containing a carbon working electrode (5 mm), carbon counter electrode and an Ag/AgCl reference electrode was screen-printed on the PET substrate, and the prepared electrode was denoted as FCE. Before FCE modification, it was activated

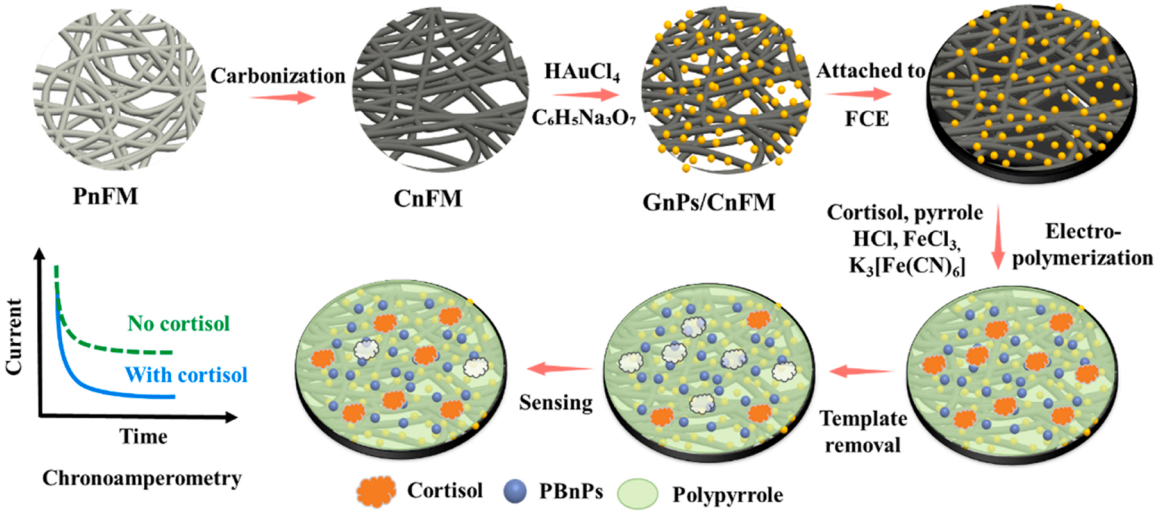

Fig. 2. Schematic diagram for preparation of PBnPs@MIP/GnPs@CnFM/FCE.

by cyclic voltammetry (CV) in 0.1 M NaOH solution under the potential ranging from 0.4 V to 1.5 V. Next, a piece of GnPs@CnFM (Fabrication processes are detailed in the Supporting Material) was attached onto the surface of FCE and dried to prepare GnPs@CnFM/FCE. Subsequently, PBnPs@MIP was electropolymerized in PBS containing 5 mM cortisol, 50 mM pyrrole, 5 mM $FeCl_3$, 5 mM $K_3[Fe(CN)_6]$ and 0.1 M HCl by applying CV from − 0.2 V to + 0.9 V with a scan rate of 50 mV s^{-1} for 10 cycles. After that, the cortisol templates were removed by CV scanning from − 0.2 V to + 0.8 V (at 50 mV s^{-1}) for 30 cycles in PBS. The prepared electrode was denoted as PBnPs@MIP/GnPs@CnFM/FCE. As a control, non-molecularly imprinted polymer modified electrode (PBnPs@NIP/GnPs@CnFM/FCE) was fabricated by the same procedure except the addition of cortisol during electro-polymerization.

2.2. Fabrication of nanofiber-based microfluidic chips

Firstly, PI/SDS nanofiber membranes were deposited on PBnPs@MIP-modified FCE by electrospinning. The collecting distance, applied voltage and solution flow rate of electrospinning were 15 cm, 9.5 kV and 1.0 μL/min, respectively. Then, PDMS ink was prepared by mixing silicone elastomer base and curing agent (*m/m* of 10/1) under stirring for 30 min, and it was stored in 4 °C for 36 h. After that, PDMS ink was directly patterned into the nanofiber membranes by direct writing. After curing, the nanofiber-based microfluidic electrochemical sensor was obtained.

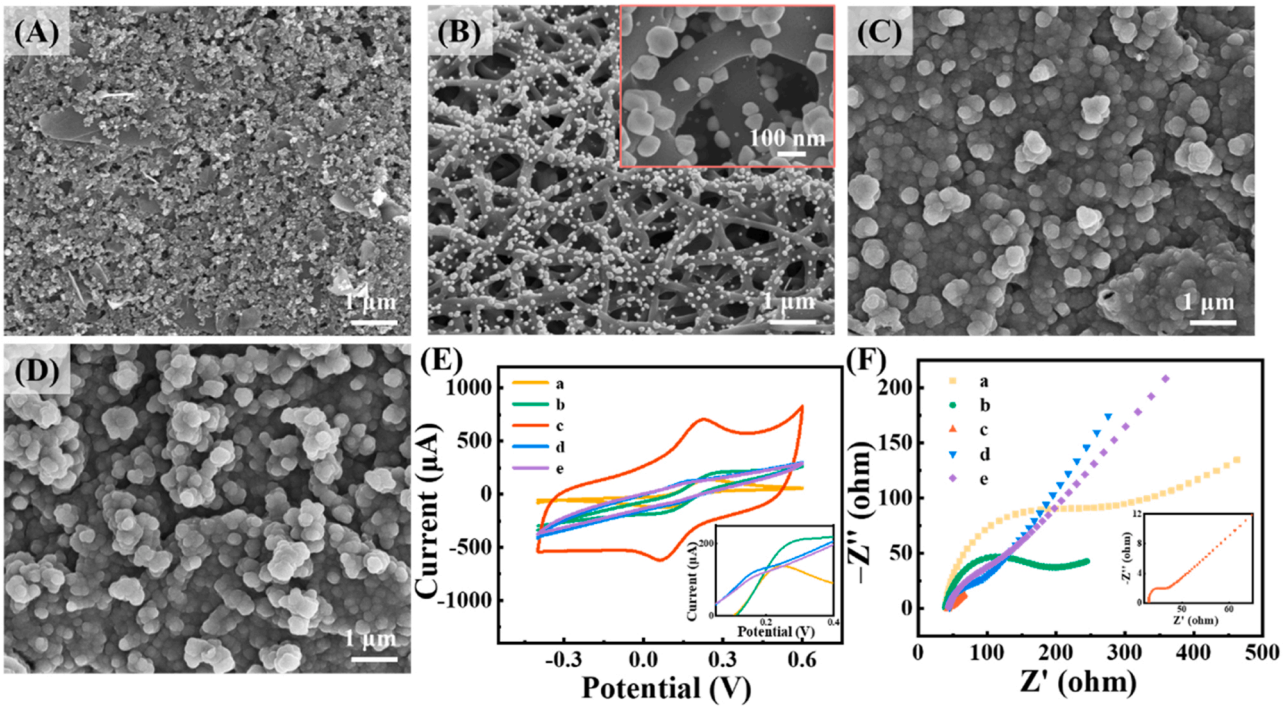

Fig. 3. Characterization of the PBnPs@MIP-modified electrode. SEM images of the PBnPs@MIP electrode at different stages, (A) bare FCE, (B) GnPs@CnFM/FCE, PBnPs@MIP/GnPs@CnFM/FCE (C) before and (D) after elution. (E) CV curves and (F) Nyquist diagrams of bare FCE (curve a), GnPs@CnFM/FCE (curve b), PBnPs@MIP/GnPs@CnFM/FCE before (curve c) and after (curve d) elution, PBnPs@MIP/GnPs@CnFM/FCE after rebinding with 1 μM cortisol (curve e) in 0.1 M KCl aqueous solution containing 5 mM $[Fe(CN)_6]^{3-/4-}$. Inset in Fig. 3E shows the magnification of anodic peak currents. The inset of (F) is the EIS plots for curve c.

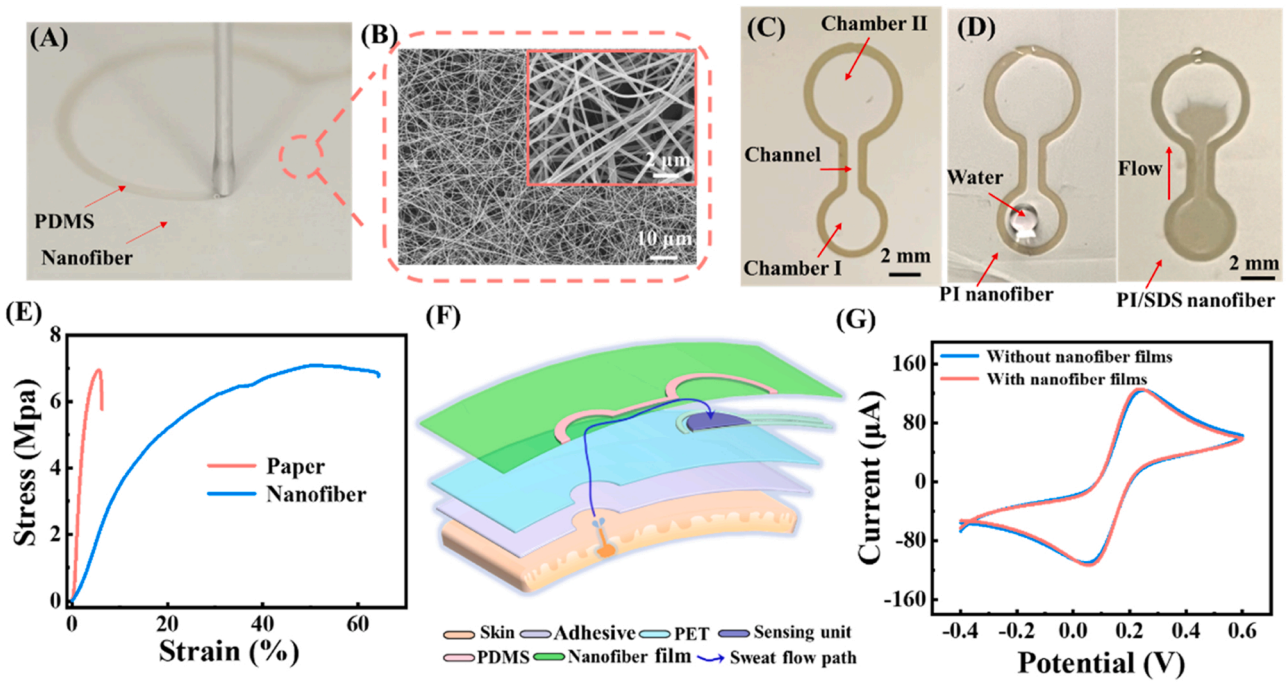

Fig. 4. Characterization of nanofiber-based microfluidic chip. (A) Photograph of writing PDMS ink on a nanofiber membrane. (B) SEM image of a PI/SDS nanofiber membrane. Inset is the corresponding image at higher magnification. (C) Photograph of a nanofiber-based chip. (D) The flow of DI water in PI nanofiber-based chip and PI/SDS nanofiber-based chip. (E) Stress–strain curves of the nanofiber membrane and paper. (F) Schematic representation of the cross-sectional view of the sensor. (G) CV curves of the electrodes in 0.1 M KCl aqueous solution containing 5 mM $[Fe(CN)_6]^{3-/4-}$.

3. Results and discussion

3.1. Design of the sensor

The reported sensor with a flexible polyethylene terephthalate (PET) as a substrate was composed of a PBnPs@MIP-modified FCE for electrochemical sensing and a nanofiber-based microfluidic chip for sweat extraction (Fig. 1A). The fabrication processes are illustrated in Fig. S1. When sweat is secreted, it passes through the inlet and is quickly absorbed by the upper microfluidic chip and automatically transmitted to Chamber II due to high hydrophilicity and porosity of nanofibrous structure of the chip. The sweat in Chamber II can work as an electrolyte, in which cortisol molecules are specifically captured by MIP, leading to occupation of the imprinting cavities. The reduction of the number of imprinted cavities hinders the electron transfer of the "built-in" probe of PBnPs, causing changes in response currents. The sensor is integrated with a flexible circuit board, which can be comfortably mounted on human body. The response signals are directly transmitted to a smartphone wirelessly via Bluetooth, and thus in situ and real-time monitoring of cortisol is realized.

3.2. Principle and characterization of the PBnPs@MIP-modified FCE

PBnPs@MIP-modified FCE was prepared by decorating GnPs@CnFM on a bare FCE electrode, followed by in situ synthesis of PBnPs@MIP via electro-polymerization (Fig. 2A). The adoption of GnPs@CnFM with porous 3D structure, large surface area and excellent electrical conductivity was conducive to promoting electron/mass transmission and enhancing sensitivity and stability of the sensor. To detect cortisol specifically, PBnPs@MIP was electropolymerized on GnPs@CnFM/FCE by using cortisol as template molecules. It's worth mentioning that PBnPs as a "built-in" redox probe were embedded into the MIP layer during electro-polymerization, allowing detection without any external probes. After removal of cortisol from GnPs@MIP by elution process, imprinted cavities were formed, offering pathways for electron/mass diffusion to PBnPs. When the cavities were re-occupied by cortisol, these accesses were blocked, and therefore the oxidation current of the inner PBnPs decreased.

Firstly, GnPs@CnFM was fabricated by electrospinning, carbonization and subsequent hydrothermal process. In Fig. S2A, the prepared PnFM has a porous and 3D network-like structure with randomly oriented PAN nanofibers, where fiber diameters are around 198 ± 32.2 nm. After carbonization, the structure remains the same as that of PnFM, while diameters of the nanofibers reduce to 174 ± 24.8 nm (Fig. S2B). Such architecture is benefit to electron/ion transfer. Raman spectra was carried out to further study the structure of the obtained CnFM. As demonstrated in Fig. S2C, the peaks around 1343 cm^{-1} for D-band and 1592 cm^{-1} for G-band are the distinct characteristic Raman shifts of carbon, revealing that carbon in fibers changes from disorder to order during carbonization. The graphitized structure in CnFM facilitates electron transfer [35,36]. To further improve the conductivity of the film, AuNPs were deposited on CnFM by a hydrothermal method. As shown in Fig S3, AuNPs with average size of 97 nm were dispersed homogeneously on the surface of each carbon nanofibers. EDS elemental mapping further confirmed the uniform distribution of GnPs on nanofiber surface (Fig. S4). The above results verify the successful preparation of GnPs@CnFM.

Next, GnPs@CnFM was attached onto FCE surface and worked as a skeleton for PBnPs@MIP electro-polymerization. The morphologies of MIP-modified FCE at different stages have been characterized using SEM (Fig. 3A-D). Compared with bare FCE (Fig. 3A), GnPs@CnFM/FCE features porous and interconnected 3D structure with homogeneous distribution of GnPs on fiber surface (Fig. 3B). Fig. S5 shows the SEM image of the Ag/AgCl reference electrode. After electro-polymerization of PBnPs@MIP, a polymer film containing lots of nanoparticles was obviously observed on GnPs@CnFM/FCE surface (Fig. 3C), while MIP without PB shows a cauliflower-like structure (Fig. S6). This result confirms the formation of MIP layer and the successful embedding of PBnPs. Subsequent elution causes the surface rougher and expose more PBnPs (Fig. 3D), which is possibly due to the removal of cortisol

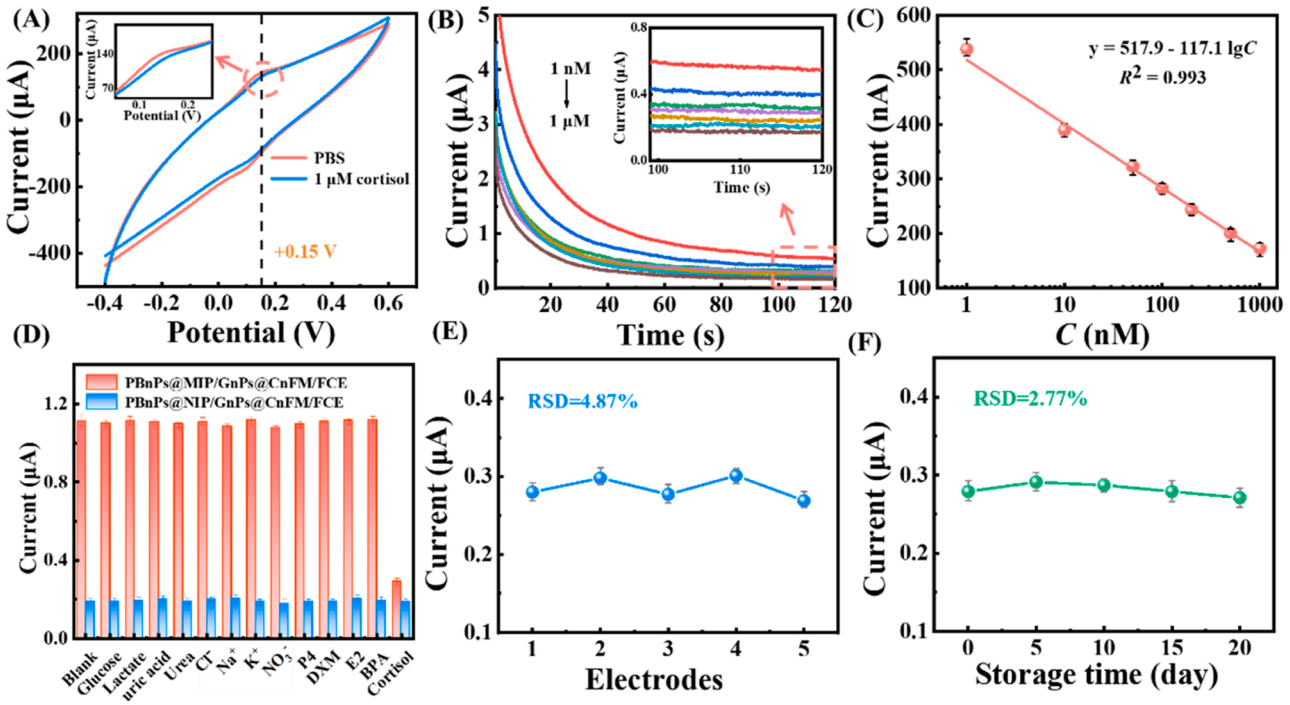

Fig. 5. Characterization of sensor performance. (A) CV of the sensor before and after binding with 1 μM cortisol in PBS containing 0.1 M KCl. Inset in Fig. 5A shows the magnification of anodic peak currents. (B) The CA response of the sensor with different cortisol concentrations (1 nM~1 μM). Inset: magnification of curves. (C) The calibration curve of the sensor. (D) CA responses of PBnPs@MIP/GnPs@CnFM/FCE and PBnPs@NIP/GnPs@CnFM/FCE towards different analytes. (E) Reproducibility and (F) long-term stability studies of the sensors. All experiments were performed for three parallel tests.

molecules. The FT-IR spectra also proved the successful preparation of the PBnPs@MIP/GnPs@CnFM/FCE (Fig. S7).

The electrochemical behaviors of electrode at different stages were tracked by CV (Fig. 3E). Compared with bare electrode (curve a), redox peak current (I_p) significantly enhanced after the modification of GnPs@CnFM (curve b) due to high electrical conductivity and porous structure of the nanomaterials. Such structure not only provides large surface area, but also is propitious to mass diffusion. After polymerization of PBnPs/MIP (curve c), I_p increased significantly, which can be attributed to the formation of conductive PPy matrix and embedded PBnPs. The increase of current is also observed from the CV curve during electro-polymerization (Fig. S8A), further confirming the enhanced conductivity of PBnPs/MIP film. After elution, due to the removal of redox precursors and over-oxidation of PPy, the redox peak currents obviously reduced (curve d) [6]. CV curves of elution process also verify the decreased redox current during scanning (Fig. S8B). When PBnPs/MIP-modified electrode was immersed in cortisol solution (curve e), its imprinting cavities were re-adsorbed with template molecules to hinder electron/ion transfer, thereby suppressing the redox current.

The electron transfer property of electrodes prepared at each step was explored by EIS. As depicted in Fig. 3F, when GnPs@CnFM was attached on electrode surface (curve b), an apparent decrease in electron transfer resistance (R_{ct}) was observed compared with that of bare FCE (curve a), in which R_{ct} decreased from 252.3 Ω to 133.4 Ω, suggesting the modification of 3D porous GnPs@CnFM benefits electron migration effectively. After PBnPs@MIP deposition (curve c), due to the formation of conductive PPy and PBNPs, R_{ct} of the modified electrode decreased further. Subsequent removal of cortisol resulted in remarkable increase in R_{ct} (curve d), which was owing to the fact that the overoxidized PPy film possesses relatively poor electric conductivity. After the sensor rebinding with cortisol, the imprinted recognition sites were occupied by cortisol again, which blocks the electron transfer of $[Fe(CN)_6]^{3-/4-}$, and thus R_{ct} elevated to 147.6 Ω (curve e). The results obtained from EIS are in good accordance with those from CV, and all of them imply the successful fabrication of PBnPs@MIP-modified sensors. Besides, several parameters for PBnPs@MIP preparation including monomer/template ratio, electro-polymerization cycle, elution cycle and incubation time were optimized to gain excellent sensing performance (Fig. S9).

3.3. Fabrication and characterization of the nanofiber-based microfluidic chip

In order to spontaneous collection and routing of sweat, a nanofiber-based microfluidic chip with strong hydrophilicity was applied to assemble with PBnPs@MIP/GnPs@CnFM/FCE. Fig. 4A shows the photograph of writing PDMS ink on the nanofiber membrane to fabricate the microfluidic chip, and the preparation process is detailed in the Supporting Material. Due to high porosity of the nanofiber membrane, PDMS ink can flow into inside of the membrane to form channels and chambers (Fig. 4B and C). Such a microfluidic chip can spontaneously transport liquid owing to the excellent hydrophilicity of PI/SDS nanofibers (Fig. 4D). Wettability test confirmed that PI/SDS nanofiber film was able to completely absorb water (Fig. S10). Furthermore, as depicted in Fig. 4E, the nanofiber membrane shows outstanding ductility with a tensile strain up to 64 %, while that for paper is only 6.3 %. Therefore, compared with paper, nanofiber membrane allows microfluidic chips to be more stretchable, enabling more conformal attachment on human skin. Moreover, the fluid velocity can be regulated by adjusting the microfluidic channel width (Fig. S11). Based on these advantages, the nanofiber-based microfluidic chip with an opening and a sensing region aligned with the inlet and the reaction chamber was directly fabricated on PBnPs@MIP/GnPs@CnFM/FCE and integrated into wearable device (Fig. 4F). When sweat is secreted, it can be immediately absorbed by the microfluidic chip through the inlet (Chamber I, 5.2 mm in diameter) and quickly transferred to the sensing region (Chamber II, 7.2 mm in diameter) along the microchannel (0.7 mm in diameter) due to the outstanding hydrophilicity of PI/SDS nanofiber film (Fig. S10). In comparison, the bottom PET substrate is less hydrophilic (Fig. S12A) and does not absorb and deliver sweat in practical usage. In the sensing region, as PBnPs@MIP/GnPs@CnFM/

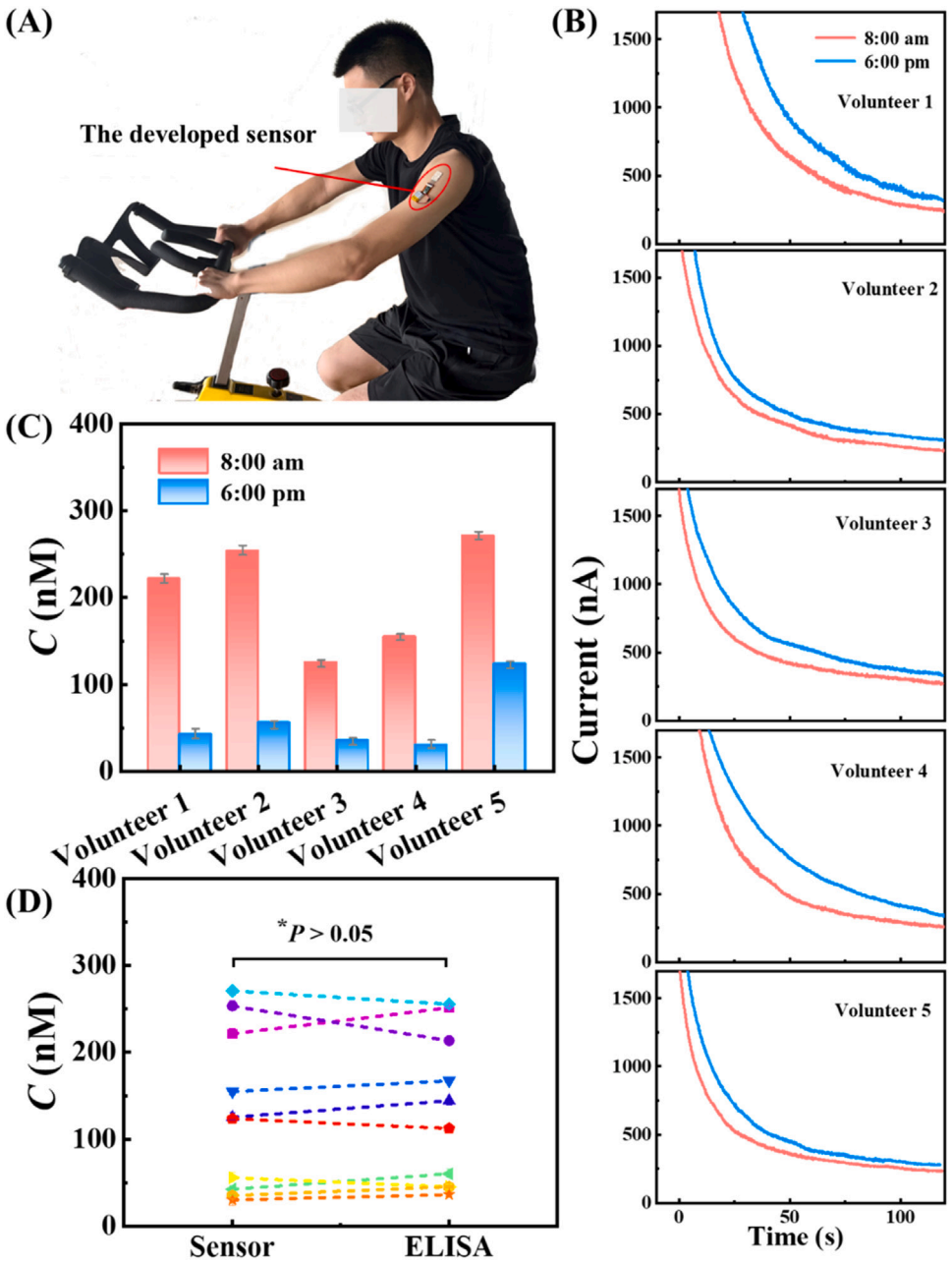

Fig. 6. On-body analysis of human perspiration. (A) Real time test of the sensor on a subject's wrist during stationary biking. (B) CA responses of the sensor for on-body measurement of cortisol from five volunteers at 8:00 a.m. and 6:00 p.m. (C) Cortisol concentrations obtained by the sensor. (D) Comparison of cortisol concentrations measured by the sensor and ELISA, $^*P < 0.05$, two-tailed *t* test.

FCE is hydrophilic (Fig. S12B) and completely soaked by sweat, sweat can act as an electrolyte, and cortisol in it can be extracted by MIP and rebind on electrode surface, thus generating response signals. It is worth mentioning that introduction of the microfluidic chip on electrode surface does not affect its electrochemical properties (Fig. 4G).

3.4. Electrochemical detection of cortisol

Under the optimal conditions, the integrated device was used to detect cortisol. As shown in Fig. 5A, a pair of redox peaks originated from the "built-in" redox probe of PB are observed in blank PBS (red curve), which show obvious decrement after incubated with cortisol (blue curve) due to occupation of imprinting cavities caused by the rebinding between cortisol and PBnPs@MIP. Since the potential of oxidation peak appeared at 0.15 V, chronoamperometry was operated at this potential to determine different concentrations of cortisol. As depicted in Fig. 5B, the response current decreases with the increase of cortisol concentration, implying that the rebound cortisol imped the electron transfer of PBnPs. A linear relationship between the response current and the logarithm of cortisol concentration was achieved from 1.0 to 1.0 × 10^3 nM in PBS with a linear regression equation of I (nA) = 517.9 − 117.1 log$C$ (nM) (R^2 = 0.993) (Fig. 5C). The detection limit was calculated to be 0.35 nM (S/N = 3), which was lower than those of most reported literatures (Table S1). Considering that the physiological level of cortisol in human sweat ranges from 0.02 to 0.5 μM [37], this device could meet the requirement of practical cortisol detection. In contrast, PBnPs@NIP electrode shows a slight response to cortisol, indicating the lack of specific recognition sites for cortisol binding (Fig. S13).

In order to evaluate specificity of the device for cortisol monitoring,

influences on common interferents in sweat were studied. Fig. 5D shows that PBnPs@MIP sensor exhibits an obvious output signal to cortisol, while negligible responses are observed in the presence of interferents. In contrast, PBnPs@NIP sensor does not demonstrate any significant difference between cortisol and interfering species. Such excellent anti-interfering ability derives from specific recognition property of PBnPs@MIP, enabling the sensor to detect cortisol in complex matrices with high accuracy. Moreover, repeatability of the sensor was examined by successive measurements of cortisol at one sensor, yielding relative standard deviation (RSD) of 3.56 % (Fig. S14). To investigate reproducibility, five different sensors prepared by the same procedures were used for cortisol detection, and the RSD was 4.87 % (Fig. 5E). For long-term stability test, the device was stored in a refrigerator at 4 °C and determined 100 nM cortisol every five days. Fig. 5F shows that the decrement in response current can be ignored, and 97.8 % of the initial signal was maintained after 20 days. In a word, the virtues in sensitivity, specificity, stability, and reproducibility allow the developed sensing device to have promising potential in actual application. The feasibility of the sensor was appraised by detecting cortisol in an artificial sweat by standard addition method. As listed in Table S2, recoveries range from 95.3 % to 104.6 % with RSDs less than 5 %, implying high reliability of the proposed sensor.

3.5. On-body sweat analysis

Flexibility is very important for wearable sensors to resist mechanical deformation caused by daily motions. As demonstrated in Fig. S15A, the electrochemical signal recovered quickly after the deformations were withdrawn, indicating admirable anti-deformation ability of the sensor regarding on-body use. Furthermore, the actual working temperature of the sensors is higher than room temperature because it is worn on the body. Fig. S15B shows that the signals of the sensors presented slight variation at 25 ℃, 37 ℃ and 40 ℃, suggesting wide temperature tolerance in on-body application.

Due to outstanding sensing performance, high mechanical and thermal stability of the developed sensor, on-body tests were carried out on five volunteers. In epidermal study, the sensor was worn on healthy volunteer's wrist during exercise on a cycle ergometer (Fig. 6A). After 18 min of exercise, sufficient sweat was accumulated in the reaction chamber, and the CA response signal was recorded after another 3 min for incubation. From Fig. 6B, the CA currents obtained from five volunteers at 8:00 am are much lower than those at 6:00 pm, indicating cortisol concentration of each volunteer secreted in the morning is greater than that in the afternoon. As depicted in Fig. 6C, the cortisol level in sweat of the five volunteers ranges from 125.2 ~ 270.6 nM in the morning while in a range of 30.1 ~ 123.4 nM in the afternoon, which is consistent with the normal concentration of cortisol in sweat (20 ~ 500 nM) [12]. In addition, ELISA was also employed to validate the prepared sensor. As shown in Fig. 6D, the data obtained by our sensor demonstrated good agreement with those from ELISA, indicating superior reliability and accuracy of the sensor and providing great potential in real-time monitoring of sweat biomarkers.

4. Conclusion

In summary, we demonstrated a flexible sensor by integrating nanofiber-based microfluidic chips for sweat sampling and PBnPs@MIP-modified FCE for electrochemical detection of cortisol. The excellent electrochemical performance of GnPs@CnFM was attributed to its high porosity and interconnected 3D structure, which acted as an ideal matrix for PBnPs@MIP polymerization and accelerated electron transfer. Thanks to the embedded PB redox probes and specificity of MIP, as well as automatic and fast sampling of the nanofiber-based microfluidic chip, the resulting device conveyed outstanding performance in terms of selectivity, rapidity, accuracy and stability for cortisol measurement in a wide detection range. Furthermore, the practical application of the developed sensor was validated by on-body test from human, and the results agreed well with those obtained from ELISA. We expect that our device will provide a versatile tactic to design wearable sensors with high accuracy and reliability for in situ and real-time monitoring of sweat biomarkers, not just cortisol.

CRediT authorship contribution statement

Xuecui Mei: Conceptualization, Methodology, Investigation, Writing-original draft. **Jiao Yang**: Formal analysis, Methodology, writing. **Xinge Yu**: Formal analysis, Manuscript revision. **Zhengchun Peng**: Methodology. **Guanghui Zhang**: Supervision, Manuscript revision. **Yingchun Li**: Project administration, Supervision, Editing, Manuscript revision.

Declaration of Competing Interest

The authors declare that they have no known competing financial interests or personal relationships that could have appeared to influence the work reported in this paper.

Data availability

Data will be made available on request.

Acknowledgments

The work financially supported by Natural Science Foundation of Shenzhen (JCYJ20200109113410174), Shenzhen Science and Technology Program (KQTD20170810105439418) and National Natural Science Foundation of China (82104121, 81973280, 82173778).

Appendix A. Supporting information

Supplementary data associated with this article can be found in the online version at doi:10.1016/j.snb.2023.133451.

References

[1] D.B. Miller, J.P. O"Callaghan, Neuroendocrine aspects of the response to stress, Metabolism 51 (2002) 5–10.
[2] E. Tu, P. Pearlmutter, M. Tiangco, G. Derose, A.J.A.O. Koh, Comparison of colorimetric analyses to determine cortisol in human sweat, ACS Omega 5 (2020) 8211–8218.
[3] G. Russell, S. Lightman, The human stress response, Nat. Rev. Endocrinol. 15 (2019) 525–534.
[4] S. Kim, B. Lee, J.T. Reeder, S.H. Seo, S.U. Lee, A. Hourlier-Fargette, et al., Soft, skin-interfaced microfluidic systems with integrated immunoassays, fluorometric sensors, and impedance measurement capabilities, Proc. Natl. Acad. Sci. USA 117 (2020) 27906–27915.
[5] A. Levine, O. Zagoory-Sharon, R. Feldman, J.G. Lewis, A.J.P. Weller, Measuring cortisol in human psychobiological studies, Physiol. Behav. 90 (2007) 43–53.
[6] W. Tang, L. Yin, J.R. Sempionatto, J.M. Moon, H. Teymourian, J.J.A.M. Wang, Touch-based stressless cortisol sensing, Adv. Mater. 33 (2021), 2008465.
[7] Y. Yu, J. Nassar, C. Xu, J. Min, Y. Yang, A. Dai, et al., Biofuel-powered soft electronic skin with multiplexed and wireless sensing for human-machine interfaces, Sci. Robot. 5 (2020), eaaz7946.
[8] Y. Song, J. Min, Y. Yu, H. Wang, Y. Yang, H. Zhang, et al., Wireless battery-free wearable sweat sensor powered by human motion, Sci. Adv. 6 (2020), eaay9842.
[9] H.-J. Jang, T. Lee, J. Song, L. Russell, H. Li, J. Dailey, et al., Electronic cortisol detection using an antibody-embedded polymer coupled to a field-effect transistor, ACS Appl. Mater. Inter 10 (2018) 16233–16237.
[10] O. Parlak, S.T. Keene, A. Marais, V.F. Curto, A.J.Sa Salleo, Molecularly selective nanoporous membrane-based wearable organic electrochemical device for noninvasive cortisol sensing, Sci. Adv. 4 (2018), eaar2904.
[11] L. Gillan, E.J.F. Jansson, P. Electronics, Molecularly imprinted polymer on roll-to-roll printed electrodes as a single use sensor for monitoring of cortisol in sweat, Biosens. Bioelectron. 206 (2022), 114142.
[12] S. Yeasmin, B. Wu, Y. Liu, A. Ullah, L.-J.J.B. Cheng, Nano gold-doped molecularly imprinted electrochemical sensor for rapid and ultrasensitive cortisol detection, Biosens. Bioelectron. 206 (2022), 114142.
[13] J.P. Herman, J.M. Mcklveen, S. Ghosal, B. Kopp, B.J.C.P. Myers, Regulation of the hypothalamic-pituitary-adrenocortical stress response, Compr. Physiol. 6 (2016) 603–621.

[14] D. Kinnamon, R. Ghanta, K.-C. Lin, S. Muthukumar, S.J.Sr Prasad, Portable biosensor for monitoring cortisol in low-volume perspired human sweat, Sci. Rep. 7 (2017) 1–13.
[15] O. Edwards, J. Galley, R. Courtenay-Evans, J. Hunter, A.J.T.L. Tait, Changes in cortisol metabolism following rifampicin therapy, Lancet 304 (1974) (549-51).
[16] S. Dalirirad, A.J.J.S. Steckl, Aptamer-based lateral flow assay for point of care cortisol detection in sweat, Sensor, Actuators B-Chem. 283 (2019) 79–86.
[17] K. Hogenelst, M. Soeter, V.J.S. Kallen, B.-S. Research, Ambulatory measurement of cortisol: where do we stand, and which way to follow? Sens. Bio-Sens. Res. 22 (2019), 100249.
[18] S.M. Mugo, J.J.A. Alberkant, Flexible molecularly imprinted electrochemical sensor for cortisol monitoring in sweat, Anal. Bioanal. Chem. 412 (2020) (1825-33).
[19] C. Cheng, X. Li, G. Xu, Y. Lu, S.S. Low, G. Liu, et al., Battery-free, wireless, and flexible electrochemical patch for in situ analysis of sweat cortisol via near field communication, Biosens. Bioelectron. 172 (2021), 112782.
[20] R.M. Torrente-Rodríguez, J. Tu, Y. Yang, J. Min, M. Wang, Y. Song, et al., Investigation of cortisol dynamics in human sweat using a graphene-based wireless mHealth system, Matter 2 (2020), 921-37.
[21] P. Manickam, S.K. Pasha, S.A. Snipes, S.J. Bhansali, A reusable electrochemical biosensor for monitoring of small molecules (Cortisol) using molecularly imprinted polymers, J. Electrochem. Soc. 164 (2017) (B54-B9).
[22] P. Gao, Y. Shen, C. Ma, et al., High-sensitivity photo-electrochemical heterostructure of the cuprous oxide-metal organic framework for a dioctyl phthalate molecularly imprinted sensor, Analyst 146 (2021) 6178–6186.
[23] J. Wang, Q. Xu, W. Xia, et al., High sensitive visible light photoelectrochemical sensor based on in-situ prepared flexible Sn3O4 nanosheets and molecularly imprinted polymers, Sens. Actuators B-Chem. 271 (2018) 215–224.
[24] X. Yang, L. Chen, X. Xiong, et al., Molecularly imprinted polymers and PEG double engineered perovskite: an efficient platform for constructing aqueous solution feasible photoelectrochemical sensor, Sens. Actuators B-Chem. 304 (2020), 127321.
[25] X. Yang, Y. Gao, Z. Ji, et al., Dual functional molecular imprinted polymer-modified organometal lead halide perovskite: synthesis and application for photoelectrochemical sensing of salicylic acid, Anal. Chem. 91 (2019) 9356–9360.
[26] W. He, C. Wang, H. Wang, M. Jian, W. Lu, X. Liang, et al., Integrated textile sensor patch for real-time and multiplex sweat analysis, Sci. Adv. 5 (2019) (eaax0649).
[27] H.Y.Y. Nyein, W. Gao, Z. Shahpar, S. Emaminejad, S. Challa, K. Chen, et al., A wearable electrochemical platform for noninvasive simultaneous monitoring of Ca2+ and pH, ACS Nano 10 (2016) 7216–7224.
[28] W. Gao, S. Emaminejad, H.Y.Y. Nyein, S. Challa, K. Chen, A. Peck, et al., Fully integrated wearable sensor arrays for multiplexed in situ perspiration analysis, Nature 529 (2016), 509-14.
[29] A. Martín, J. Kim, J.F. Kurniawan, J.R. Sempionatto, J.R. Moreto, G. Tang, et al., Epidermal microfluidic electrochemical detection system: enhanced sweat sampling and metabolite detection, ACS Sens. 2 (2017) 1860–1868.
[30] J. Choi, D. Kang, S. Han, S.B. Kim, J.A.J.Ahm Rogers, Thin, soft, skin-mounted microfluidic networks with capillary bursting valves for chrono-sampling of sweat, Adv. Healthc. Mater. 6 (2017), 1601355.
[31] Z.M. Sheng Li, Zhonglin Cao, Lijia Pan, Yi Shi, Advanced wearable microfluidic sensors for healthcare monitoring, Small 16 (2020), e1903822.
[32] J. Xiao, Y. Liu, L. Su, D. Zhao, L. Zhao, X.J. Zhang, Microfluidic chip-based wearable colorimetric sensor for simple and facile detection of sweat glucose, Anal. Chem. 91 (2019) 14803–14807.
[33] Y. Ding, H. Hou, Y. Zhao, Z. Zhu, H. Fong, Electrospun polyimide nanofibers and their applications, Prog. Polym. Sci. 61 (2016) 67–103.
[34] J. Liang, H. Zhao, L. Yue, G. Fan, T. Li, S. Lu, et al., Recent advances in electrospun nanofibers for supercapacitors, J. Mater. Chem. A 8 (2020), 16747-89.
[35] X. Wei, M. Zhu, J. Li, L. Liu, B.J.N.E. Ding, Wearable biosensor for sensitive detection of uric acid in artificial sweat enabled by a fiber structured sensing interface, Nano Energy 85 (2021), 106031.
[36] J. Yang, Z. Yan, D.Y.J.C. Kim, Electrochemical sensing performance of nanodiamond-derived carbon nano-onions: Comparison with multiwalled carbon nanotubes, graphite nanoflakes, and glassy carbon, Carbon 98 (2016) 74–82.
[37] A.J. Steckl, P.J.A.S. Ray, Stress biomarkers in biological fluids and their point-of-use detection, ACS Sens. 3 (2018) 2025–2044.

Xuecui Mei is pursuing his Ph.D. degree in the College of Science, Harbin Institute of Technology (Shenzhen). His research is focused on wearable biosensor.

Jiao Yang received her B.S. from Harbin Institute of Technology in 2009, and Ph.D. study in Sungkyunkwan University in 2015. She continued her postdoctoral fellow at School of Science, Harbin Institute of Technology (Shenzhen). Her research is focused on synthesis of nanomaterial and electrochemical biosensor.

Xinge Yu: received his B.S. in engineering and technology in optoelectronics from the University of Electronic Science and Technology of China (UESTC) in 2009. He finished his Ph.D. research in solution process/printable flexible electronics at Northwestern University under the supervision of Prof. Tobin J. Marks and Prof. Antonio Facchetti, and recived his Ph.D. degree in Optical Engineering from UESTC in 2015. From 2015–2018, Xinge Yu was a postdoctoral research associate in the Center for Bio-Integrated Electronics at Northwestern University and an adjunct research assistant professor in the Department of Materials Science and Engineering at the University of Illinois at Urbana-Champaign, where he was working on novel flexible and bio-electronics with Professor John A. Rogers.

Zhengchun Peng: received his Ph.D. degree from Georgia Institute of Technology (America) in 2010. Then he worked as a postdoctoral researcher at Emory University (America). In 2015, he joined Shenzhen University (Shenzhen, China). His research interests focus on Micro/nano sensors, electronic skin, machine touch and tactile feedback.

Guanghui Zhang is a deputy chief doctor of Shenzhen Hengsheng Hospital. He received his B.S. for Xinxiang Medical College. He is good at clinical test technology operation and laboratory data analysis of difficult cases.

Yingchun Li received her B.S. from Shihezi University in 2003, and M.S. from Xi'an Jiaotong University in 2006. She continued her Ph.D. study in Halle University in Germany and received her doctor degree in 2011. Then she joined Shihezi University as one scientist of the "Recruitment Program of Global Experts". Now, Prof. Li continued her research in Harbin Institute of Technology (Shenzhen), and her research field is in development of advanced functional materials and sensors for serving pharmaceutical and biomedical analysis.